Multi-criterion 3D Segmentation and Registration of Pulmonary Nodules on CT: A Preliminary Investigation*

William Mullally, BA,[a] Margrit Betke, PhD,[a] Harrison Hong, BA,[a] Jingbin Wang, MEng,[a] Katelyn Mann,[a] and Jane P. Ko, MD[b]

[a] Computer Science Department, Boston University, Boston, MA, USA,
[b] Department of Radiology, New York University, New York, NY, USA

ABSTRACT

We developed multi-criterion nodule segmentation and registration methods that facilitate identification of corresponding nodules in sequential chest computed tomography (CT) scans. Our segmentation algorithm automatically determines regions of interest and segments nodules according to density and shape constraints. Our registration algorithm matches nodules based on an affine registration of lung surfaces, combined with nodule size, location, shape, and exclusivity measures. We tested the accuracy of our results on sequential CT scans taken of patients for clinical purposes by comparison to those found by a radiologist.

Keywords: Chest CT, Lung Cancer, Pulmonary Nodules, Segmentation, Registration, Computer-Aided Diagnosis

1. Introduction

Chest CT is used to diagnose pulmonary metastasis of oncology patients and evaluate disease progression or regression during treatment. Low-dose CT is currently being evaluated as a possible screening method for high-risk individuals to identify early lung cancer. Lung cancer remains the leading cause of cancer death in the United States, killing 160,000 people a year. The overall 5-year survival rate is 15%, but early detection and resection can improve the prognosis significantly. For example, the 5-year survival rate for Stage I cancer is 67% [9]. A large number of patients undergoing screening for lung cancer have non-calcified nodules; 50% of the nodules are less than 5 mm in diameter [5]. Such small nodules are difficult to characterize, because they are commonly benign but may also represent early malignancy [5]. Small nodules are therefore followed over time to determine potential size changes and evaluate growth rates. Computer assistance has been proposed to handle inter- and intra-observer variations and also to decrease error in measurements [10].

Several techniques for automated nodule segmentation in the lung have been suggested [1, 3, 4, 7, 8, 11]. One common approach is to segment nodules based on thresholds imposed on the density values within CT images [7]. Template-based

*Financial support by the Whitaker Foundation, National Science Foundation, Office of Naval Research, and National Institutes of Health is gratefully acknowledged.

methods have been used [8]. We advance an algorithm which uses geometric information, first proposed by [11]. Many approaches require manual assistance to select an area containing a nodule [6, 11].

Our approach uses three-dimensional (3D) density and shape information and automatically selects regions of interest in which nodule candidates lie. We also developed a registration algorithm which finds nodule correspondence in successive CT scans. We initially align nodules by applying the same registration parameters that optimally align lung surfaces [2]. Nodule correspondence is then found by using nodule distance, size, location, shape, and exclusivity measures. We use these geometric measures because the affine registration of lung surfaces alone is not sufficient to find correct correspondence due to the non-rigid nature of the lung and the density variations of structures in the lung. We tested our methods on a pair of successive CT scans of a patient with a small number of nodules.

2. Materials and Methods

2.1. Automatic Nodule Segmentation

We call contiguous regions of soft tissue voxels in the lung "nodule candidates." Nodule candidates are 3D regions that can be identified by imposing a threshold on the density value at each voxel. We use an initial threshold to identify potential nodules in the lung and then use two measures, differences in 3D density values along the nodule border and sphere occupancy, to refine our segmentation. These measures are observed in a range of thresholds and serve as a basis for choosing the optimal threshold with which to segment a nodule candidate.

2.1.1. Nodule Candidate Identification

Voxels belong to the same nodule candidate if they are 4-connected to other voxel nodule candidates in the same axial slice. Voxels on different slices are connected if they are adjacent in the slices immediately above or below.

Nodule candidates are initially identified by using a fixed threshold T_I throughout the entire lung. All voxels with a value greater than T_I are considered for nodule candidacy, and a filter is applied to remove small isolated groups of pixels from consideration.

2.1.2. Density Difference Measure

We generalize the two-dimensional measure of "gradient strength" proposed by Zhao et al. [11] to three dimensions and call it "contour strength." We define it as the average magnitude of density differences across the nodule contour for every voxel on the nodule candidate's contour. The contour of a nodule candidate contains all voxels which have at least one neighbor that is not part of the nodule candidate. This neighborhood is defined by six connections in three dimensions.

At each voxel V_i under consideration, if a voxel V_j on one side of V_i is part of the nodule candidate and the voxel V_k on the opposite side of V_i is not part of the nodule candidate, then the contour strength of V_i is defined as the average of the absolute values of density differences between all such pairs of opposing voxels V_j and V_k. There are thirteen such possible pairs around each voxel V_i.

2.1.3. Sphere Occupancy Measure

We define the radius r of a nodule candidate to be the distance from that nodule's centroid to its furthest point. Given the volume V of the nodule candidate, we define the sphere occupancy of the object as

$$c = \frac{3V}{4\pi r^3}, \tag{1}$$

where $0 < c \leq 1$. A nodule with spherical shape has an occupancy value close to one. We set $c_{\mathrm{min}} = 0.25$ as a desirable lower bound on the occupancy value of a nodule.

2.1.4. Determining Optimal Segmentation

To find an optimal threshold T_{opt}, we compute both the maximal contour strength and the sphere occupancy of the nodule candidate over a range of n threshold levels $T_1, \ldots, T_n$, beginning at the lowest value $T_1 = T_I$. The threshold T_k that contains the maximal contour strength is considered first. If the object has a sphere occupancy value greater than c_{min} at T_k, then $T_{\mathrm{opt}} = T_k$. Otherwise a sequence of increasingly higher thresholds is checked until a threshold is found at which the object has a sphere occupancy value greater than c_{min}. If no threshold satisfies this constraint, the threshold at which the highest sphere occupancy was found is considered to be T_{opt}.

2.1.5. Nodule Matching

We initially align objects in the lung by applying the same registration parameters that optimally align lung surfaces. The nodules we are trying to match can vary greatly in size and shape over time, so size and shape criteria for matching must necessarily be weak. We reject for match consideration nodules which are grossly mismatched in size and shape. To better match nodules we can also use the fact that some nodules move in relation to other structures in the lung. Therefore we compare nodule distances to the lung surface. We score the strength of individual nodule matches by adding the distance between nodule centroids to the magnitude of the difference in nodule distances to the lung wall. The lowest scores indicate the best match. We also impose an exclusivity constraint in which we allow for the possibility of new nodules appearing and previously imaged nodules disappearing, but in which two nodules can not correspond to the same nodule in consecutive scans.

3. Results

We tested the accuracy of our methods on two successive CT scans of a patient taken for clinical purposes. These scans contain a complicated topology of structures, such as nodules and vessels. We can test how this topology affects nodule segmentation and matching. We compared our results to those found by a radiologist.

We tested our segmentation method on eight nodules, four from each of the two scans. We also compare our segmentation results to those found by a similar method proposed in [11] which uses 2D measures. We substitute our automatic region-of-interest method for Zhao et al's interactive region-of-interest selection mechanism.

If we allow thresholds that are too large, it is likely to create very small objects that will satisfy the sphere occupancy constraint and produce an incorrect segmentation. For this reason we restricted the range of threshold values from $T_1 = -500$ HU to $T_n = 0$ HU in steps of 25 HU.

In Table 1, we show that our method generally has a higher correspondence to the hand segmented nodules than does the 2D method. In addition, as can be seen in Fig. 1, the 2D method can fragment a nodule when applied to a spiculated object. Our 3D method avoids this problem. Other segmentations can be seen in Fig. 2.

Table 1
Volumes of Segmented Nodules and Overlap with Hand-Segmented Nodules (in Units of Voxels)

Nodule No./Case	Radiologist Volume	2D Volume	2D Overlap	3D Volume	3D Overlap
1–1	218	574	73	527	149
1–2	260	490	89	579	207
2–1	106	78	16	75	53
2–2	126	105	68	80	70
3–1	52	28	28	36	36
3–2	48	56	41	56	44
4–1	482	559	357	563	354
4–2	538	412	387	415	377

In testing our nodule matching algorithm we assumed that the four nodules had been identified in the first scan, but not in the second. We correctly detected the nodules in the second scan. The nodules were far apart in space and were unlikely to be mismatched with each other, but several hundred other objects (mostly vessels) were segmented and were considered in the matching process.

Figure 1. Segmentation Results for Nodule 1–2. Radiologist (left), 2D Method (middle), 3D Method (right).

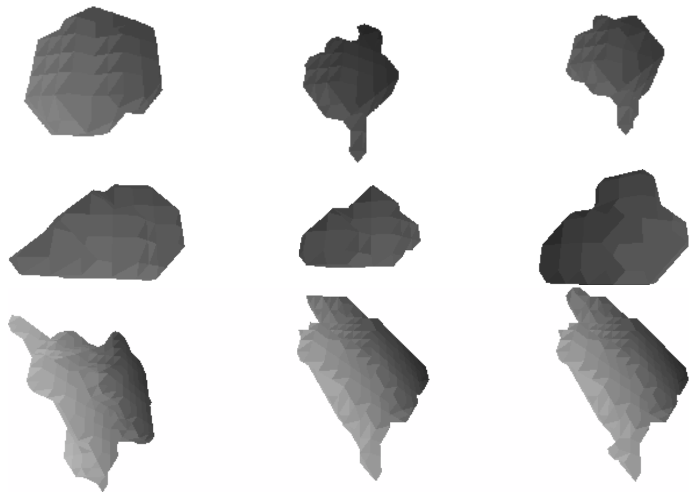

Figure 2. Segmentation Results for Nodules 2–1, 3–1, 4–1. Radiologist (left), 2D Method (middle), 3D Method (right).

4. Discussion and Conclusions

In the cases we examined, all nodules correctly matched even when judged solely on the bases of their initial affine alignment. However, the additional geometric criteria we used, are important for three reasons. First, the distance between some of the nodule locations after the affine registration was high. In general, such a large distance could produce mismatches since closer structures may exist. Second, imposing a constraint on the range of possible volumes ruled out many of the second and third choice matches, indicating that this constraint will be useful in the general case. Third, matched nodules had high similarities in their distances to the lung wall and little similarity to the distances to the lung wall of surrounding structures.

In summary, we have developed an automatic multi-criterion segmentation algorithm to segment nodules in CT images. The algorithm uses three-dimensional density and shape information to extract nodules. Our method avoids some problems that previous methods encounter. Most importantly, our segmentation method is accurate enough to establish correct correspondence between nodules in successive CT scans. By segmenting nodules and automatically finding nodule correspondence in successive CT scans, we hope to facilitate a radiologist in the evaluation and comparison of pulmonary nodules on sequential patient chest CT scans.

REFERENCES

1. S. G. Armato, M. L. Giger, C. J. Moran, J. T. Blackburn, K. Doi, and H. MacMahon. Computerized detection of pulmonary nodules on CT scans. *Radiographics*, 19:1303–1311, 1999.

2. M. Betke, H. Hong, and J. P. Ko. Automatic 3D registration of lung surfaces in computed tomography scans. In W. J. Niessen and M. A. Viergever, editors, *Medical Image Computing and Computer-Assisted Intervention – MICCAI 2001: 4th International Conference*, pages 725–733, Utrecht, The Netherlands, October 2001. Springer-Verlag, Berlin.
3. M. S. Brown, M. F. McNitt-Gray, N. J. Mankovich, J. G. Goldin, J. Hiller, L. S. Wilson, and D. R. Aberle. Method for segmenting chest CT image data using an anatomical model: Preliminary results. *IEEE Trans Med Imag*, 16(6):828–839, December 1997.
4. M. L. Giger, K. T. Bae, and H. MacMahon. Computerized detection of pulmonary nodules in computed tomography images. *Invest Radiol*, 29(4):459–465, 1994.
5. C. I Henschke, D.I. McCauley, D. F. Yankelevitz, D. P. Naidich, G. McGuinness, O. S. Miettinen, D. M. Libby, M. W. Pasmantier, J. Koizumi, N. K. Altorki, and J. P. Smith. Early lung cancer action project: overall design and findings from baseline screening. *Lancet*, 354(9173):99–105, July 1999.
6. Y. Kawata, N. Niki, H. Ohmatsu, M. Kusumoto, R. Kakinuma, and K. Mori et al. Analysis of pulmonary nodule evolutions using a sequence of three-dimensional thoracic CT images. In *Medical Image Computing and Computer-Assisted Intervention (MICCAI)*, pages 103–110, Utrecht, The Netherlands, Oct. 2001.
7. J. P. Ko and M. Betke. Chest CT: Automated nodule detection and assessment of change over time – preliminary experience. *Radiology*, 218(1):267–273, 2001.
8. Y. Lee, T. Hara, H. Fujita, S. Itoh, and T. Ishigaki. Automated detection of pulmonary nodules in helical CT images based on an improved template-matching technique. *IEEE Trans Med Imag*, 20(7):595–604, July 2001.
9. C. F. Mountain. Revisions in the international system for staging lung cancer. *Chest*, 111(6):1710–1717, June 1997.
10. D. F. Yankelevitz, R. Gupta, B. Zhao, and C. I. Henschke. Small pulmonary nodules: evaluation with repeat CT – preliminary experience. *Radiology*, 212(2):561–566, 1999.
11. B. Zhao, D. Yankelevitz, A. Reeves, and C. Henschke. Two-dimensional multi-criterion segmentation of pulmonary nodules on helical CT images. *Med Phys*, 26(6):889–895, 1999.